

Video Article

# Observation of the Ciliary Movement of Choroid Plexus Epithelial Cells *Ex Vivo*

Takafumi Inoue<sup>1</sup>, Keishi Narita<sup>2</sup>, Yuta Nonami<sup>1</sup>, Hideki Nakamura<sup>1</sup>, Sen Takeda<sup>2</sup>

<sup>1</sup>Department of Life Science and Medical Bioscience, Faculty of Science and Engineering, Waseda University

<sup>2</sup>Department of Anatomy and Cell Biology, Interdisciplinary Graduate School of Medicine & Engineering, University of Yamanashi

Correspondence to: Takafumi Inoue at [inoue.t@waseda.jp](mailto:inoue.t@waseda.jp), Sen Takeda at [stakeda@yamanashi.ac.jp](mailto:stakeda@yamanashi.ac.jp)

URL: <https://www.jove.com/video/52991>

DOI: [doi:10.3791/52991](https://doi.org/10.3791/52991)

Keywords: Neurobiology, Issue 101, motile cilia, fast video microscopy, scanning electron microscopy, choroid plexus epithelial cells, motion tracking, video-enhanced contrast-differential interference contrast

Date Published: 7/13/2015

Citation: Inoue, T., Narita, K., Nonami, Y., Nakamura, H., Takeda, S. Observation of the Ciliary Movement of Choroid Plexus Epithelial Cells *Ex Vivo*. *J. Vis. Exp.* (101), e52991, doi:10.3791/52991 (2015).

## Abstract

The choroid plexus is located in the ventricular wall of the brain, the main function of which is believed to be production of cerebrospinal fluid. Choroid plexus epithelial cells (CPECs) covering the surface of choroid plexus tissue harbor multiple unique cilia, but most of the functions of these cilia remain to be investigated. To uncover the function of CPEC cilia with particular reference to their motility, an *ex vivo* observation system was developed to monitor ciliary motility during embryonic, perinatal and postnatal periods. The choroid plexus was dissected out of the brain ventricle and observed under a video-enhanced contrast microscope equipped with differential interference contrast optics. Under this condition, a simple and quantitative method was developed to analyze the motile profiles of CPEC cilia for several hours *ex vivo*. Next, the morphological changes of cilia during development were observed by scanning electron microscopy to elucidate the relationship between the morphological maturity of cilia and motility. Interestingly, this method could delineate changes in the number and length of cilia, which peaked at postnatal day (P) 2, while the beating frequency reached a maximum at P10, followed by abrupt cessation at P14. These techniques will enable elucidation of the functions of cilia in various tissues. While related techniques have been published in a previous report<sup>1</sup>, the current study focuses on detailed techniques to observe the motility and morphology of CPEC cilia *ex vivo*.

## Video Link

The video component of this article can be found at <https://www.jove.com/video/52991/>

## Introduction

Cilia are hair-like projections on the surface of most vertebrate cells, which have attracted attention by medical researchers because of a class of diseases termed ciliopathies<sup>2–4</sup>. Despite the ubiquitous expression of the organelle, a wide variety of ciliary functions have been reported, including motility and biosensing. For example, motile cilia on the mucoepithelial surface transport mucus<sup>5</sup> and epithelial debris to the outlet of tracts, thereby preventing disease by clearing the surface of epithelia. Moreover, during early developmental periods and embryonic stages, cilia regulate the proliferation of stem cells<sup>6</sup>, and are involved in the determination of left–right asymmetry of the vertebrate body<sup>7</sup>.

Choroid plexus epithelial cells (CPECs) are derivatives of neuroepithelial cells that cover the surface of the choroid plexus tissue in the brain, which play important roles in maintaining homeostasis of the intracranial environment by production of cerebrospinal fluid (CSF). It has been previously demonstrated that CPECs have multiple non-motile cilia that regulate the production of CSF through G-protein-coupled receptors that are specifically concentrated on the cilia<sup>8</sup>. Although these cilia had been regarded as quiescent non-motile cilia, it was discovered that some CPEC cilia exhibit transient motility during the neonatal period<sup>1</sup>. This finding was quite important because it revealed that so-called non-motile cilia are not necessarily immotile from the beginning of development and might display transient motility during specific time windows, possibly in response to specific physiological demands and functions<sup>9</sup>. To precisely describe the motile nature of CPEC cilia, it is necessary to develop an *ex vivo* observation system that encompasses analysis of the kinetic profiles unique to CPEC cilia.

With respect to motility, although several technical reports have described observations of the motile cilia of the tracheal epithelium<sup>5,10</sup>, motile single-cell flagella<sup>11</sup>, so-called conventional motile cilia<sup>12</sup>, and nodal cilia<sup>13</sup>, detailed analytical methods applicable to relatively undulated structures such as the choroid plexus have not been well documented so far. Moreover, a high time resolution is required to analyze the ciliary movement of CPECs, in which expensive high-speed cameras are indispensable. To circumvent this necessity and simplify monitoring the ciliary motility of various cell types, a low cost, high-speed camera has been introduced, and an easily accessible and convenient method to record the motility of motile cilia, especially to describe the speed and pattern of motion of each cilium, has been developed<sup>1</sup>. Moreover, original image analysis software “TI Workbench” has been used here to facilitate detailed analysis of motility. Collectively, this method provides a new concise strategy to analyze ciliary motion together with correlative scanning electron microscopy (SEM), which can be adopted in a wide range of cilium research.

## Protocol

The protocols and use of experimental animals were approved by the institutional animal care and use committees at the University of Yamanashi and Waseda University. Animal care was performed in accordance with institutional guidelines.

### 1. CPEC Preparation

1. Prepare the following apparatuses and materials: a stereo microscope, preferably capable of transmitting illumination from the bottom; a pair of watchmaker forceps (Dumont #3 or #4), flame-sterilized, straight operating scissors, flame-sterilized; two sterile 10 cm plastic dishes containing 20 ml ice-cold Leibovitz L-15 medium; 35 mm glass-bottom dishes containing 2 ml RT Leibovitz L-15 medium; a 100 ml beaker containing 70% ethanol; neonatal mouse pups.
2. Briefly immerse a neonatal mouse in 70% ethanol and euthanize quickly by decapitation using the operating scissors.
3. Place the head immediately in ice-cold Leibovitz L-15 medium in the sterile 10 cm dish.
4. Remove the skin from the calvaria using the pair of watchmaker forceps, cut open the skull to expose the brain, and then cut the cranial nerves to isolate the whole brain.
5. Transfer the brain to a new dish containing ice-cold Leibovitz L-15 medium and observe under the stereo microscope, making sure that the brain is completely immersed in the medium.
6. Set the dorsal aspect of the brain facing up, and orient the brain so that the olfactory bulbs reside at the three o'clock position (for right-handed persons). Hold the brain gently with the forceps in the left hand.
7. Using the fine dissection forceps (Dumont #3 or #4) in the right hand, cut the corpus callosum and underneath the parenchyma connecting the cerebral hemispheres, along the longitudinal fissure of the cerebrum.
8. Gently push the cerebral hemispheres away to the lateral sides and expose the transverse cerebral fissure.
9. Separate the hemispheres by pinching out the parenchyma between the hemisphere and thalamus.
10. Gently pull out the lateral ventricular choroid plexus that is attached to the lateral side of the hippocampus by the lamina affixa.
11. Transfer the isolated choroid plexus to the 35 mm glass-bottom dish containing fresh Leibovitz L-15 medium, and overlay a weight (Materials List) gently to hold the tissue in place.

### 2. Live Imaging of CPEC Cilia

1. Confirm proper ultraviolet (UV) and infrared (IR) cut filter(s) to block light shorter than 400 nm and longer than 700 nm, and that neutral density (ND) filters (25% and 6%) are inserted in the light path of the inverted microscope.
2. Adjust the focus of the objective lens roughly by eye, and then adjust the condenser so that the center and focus to conform to the Köhler illumination. Insert an appropriate differential interference contrast (DIC) prism, a DIC element, as well as analyzer and polarizer elements in the light path to conform to the DIC optics.
3. Adjust the contrast of view by the DIC prism position so that the structure of the tissue surface is most recognizable. If all cilia of the target cells are motile, a clear view of motile cilia cannot be obtained by eye because of their movement.
4. Change the light path to the video camera, and remove the ND filters to increase the light power.
5. Use the camera in focusing mode to adjust the field of view and focus. During focusing, in which video images are displayed at real-time on the monitor, a clear view of motile cilia is not available.
6. Use the camera at 200 Hz with an exposure time of 0.1 msec for the desired period (seconds to minutes). After acquisition of the image stack, single frames will display clear ciliary structures. If ciliary edges are blurred, increase the frame rate or use a shorter exposure time.
7. Record the motion of CPEC cilia within 25–60 min after euthanasia in Leibovitz L-15 medium.

### 3. Analysis of Ciliary Motion

1. Manually track beating patterns of each cilium on the computer monitor. Mark ciliary tip positions in each frame with the mouse pointer, which are assembled for trajectory information of each cilium. Either analyze the trajectory information using the same software or export to other more general applications for further analysis. The efficiency of this analysis step is described in the Discussion.
2. Classify the trajectories into two modes of motion, back-and-forth or rotational, by eye.
3. Calculate the ciliary beating frequency (CBF) using the following formula:  $[CBF = (\text{number of frames per second}) / (\text{average number of frames for a single beat})]^{14}$ , which can be obtained from a ciliary tip motion diagram (**Figure 3**). Repeat this calculation for multiple ciliary beating cycles, because other cilia on the same cell can interfere with the motion of each cilium, resulting in irregularity.
4. To analyze the angular uniformity of the ciliary beating axes within a single cell, define the beating angle  $\theta$  for each trajectory (**Figure 4**). For back-and-forth trajectories, fit the positions of the cilia tip to a straight line, and define  $\theta$  as the angle the line makes with x-axis. For rotational trajectories, fit the positions to an ellipse, and define  $\theta$  as the angle the major axis of the ellipse makes with x-axis. Details of the fitting are described in the Representative Results section.
5. For quantitative description of each trajectory, calculate generalized aspect ratio  $AR$ . Briefly, rotate the trajectory by  $-\theta$  and define  $AR$  as the ratio between the widths of the distribution along x- and y-axes (**Figure 4B**). Details are shown in the Representative Results section, and the interpretation, significance, and the limitation of the parameter are described in the Discussion.

### 4. Sample Preparation for SEM

Note: SEM is an important method to evaluate the status of cilia on CPECs in a comprehensive manner. To prepare specimens for SEM, a standard procedure reported previously<sup>15</sup> is employed with slight modifications.

1. Before dissecting the tissue from the brain, prepare the fixative in a 5 ml glass vial with a polyethylene cap. The fixative consists of 2% paraformaldehyde, 2.5% glutaraldehyde (half Karnovsky's solution<sup>16</sup>) in 0.1 M phosphate buffer, pH 7.4.
2. Dissect out the tissue from the brain as described in step 1.
3. Briefly rinse the isolated tissue with Hank's balanced salt solution (HBSS) in a new dish and then fix the tissue in the fixative in the glass vial for 1 hr at room temperature. Use disposable transfer pipettes and handle the specimens gently. After rinsing in HBSS, the tissue becomes sticky.
  1. To transfer the specimens into the fixative solution, slowly expel a small amount of solution containing the tissue from the transfer pipette as a droplet and add to the fixative.
4. After fixation, discard the fixative and rinse the tissue with phosphate buffer three times.
5. Immerse the tissue in a 10% sucrose solution to wash out the remaining aldehydes. To ensure complete elimination of aldehydes, immerse the samples in the solution for 10 min and then repeat twice with fresh 10% sucrose. This step is important to achieve proper post-fixation in subsequent steps.
6. Immerse the tissue in a solution of 1% osmium tetroxide in phosphate buffer for 30 min and then place on ice for post-fixation. Judge the degree of osmification by the sample color: when aldehydes are completely removed, the sample is black.
7. Wash the post-fixed tissue samples extensively with double distilled water several times.
8. Dehydrate the samples by immersion in graded concentrations of ethanol, usually 65%, 75%, 85%, 95%, 99%, and 100%, for 10 min each. Obtain anhydrous ethanol by placing molecular sieves into 99.5% ethanol from a newly purchased bottle. Repeat dehydration with anhydrous ethanol three times.
9. Place the dehydrated samples into isoamyl acetate, a substitution reagent for critical point drying, for 10 min. Repeat this step twice. This reagent evaporates rapidly and the sample can become dry, resulting in destruction by surface tension. Therefore, do not dry the sample completely.
10. After the final exchange of isoamyl acetate, remove most of the solvent, immediately wrap the open glass vial with aluminum foil, and place the vial on dry ice. Using a needle or fine forceps, make several holes in the foil covering the mouth of the vial, so that liquid carbon dioxide flows easily into the vial in the critical point dryer. Proceed to the next step as quickly as possible.
11. In this step, minimize the carryover of isoamyl acetate into the chamber of the dryer, but do not let the sample dry out completely before critical point drying. In addition, do not leave the sample on dry ice for an unnecessarily long time to avoid the formation of frost on the vial.
12. Transfer the foil-wrapped glass vials containing the tissue samples into the critical point dryer that ensures the surface structure of the tissue remains intact while removing water contained in the tissue. Detailed information on operating the critical point dryer can be obtained from the manufacturer's instructions.
13. Handle the samples carefully using a toothpick to minimize mechanical damage. The resulting dried tissue samples are fragile. Mount the samples on metal stubs and coat with gold-palladium using an ion sputter.

## 5. Observation by SEM

1. Observe by SEM and record images with a digital camera equipped to scanning electron microscope.
2. Transfer digital image data to a PC for analysis.

## Representative Results

An overview of the workflow is shown in **Figure 1**, including images of the devices.

Live motion observations of CPECs

**Movie 1** shows a movie of CPECs isolated from a perinatal mouse, and **Movie 2** shows an expanded view of the images in **Movie 1**. It should be noted that individual ciliary tips are less clear in still images compared with those in movies. **Figure 2** shows tracking of the motion of two cilia with different modes of movement, back-and-forth and rotational movements, from the data shown in **Movies 1** and **2**. **Figure 3** shows a simple analysis of the trajectories of the cilia, in which the phase difference in the two coordinates is obvious in the rotational movement.

Analysis of CPEC ciliary tip trajectories

Detailed methods to quantitatively analyze each trajectory are shown in **Figure 4** with schematic illustrations of the beating angle  $\theta$  definitions (A) and a flow chart of the analysis with representative results (B).

To define the beating angle  $\theta$  for back-and-forth trajectories, fit the positions of the ciliary tip during multiple cycles to a straight line  $y = ax + b$ , and define the beating direction as that along the fitted line. Define the beating angle here as  $\theta = \text{Arc tan } a$ . Because line fitting often fails to extract the direction in cases of rotational movement, fit the rotational trajectories to an ellipse, and define the direction as that along the long axis of the fitted ellipse. More precisely, the tip positions  $(x, y)$  during multiple beating cycles are fitted to the function below.

$$\left( \frac{x' - x_0}{r_{\text{long}}} \right)^2 + \left( \frac{y' - y_0}{r_{\text{short}}} \right)^2 = 1, (r_{\text{long}} > r_{\text{short}})$$

where

$$\begin{aligned} x' &= x \cdot \cos \theta + y \cdot \sin \theta, \\ y' &= -x \cdot \sin \theta + y \cdot \cos \theta \end{aligned}$$

The ellipse fitting involves five fitting parameters:  $x_0$ ,  $y_0$ ,  $a$ ,  $b$ , and  $\theta$ . The  $x$ - and  $y$ -spatial coordinates of the center of the ellipse are  $x_0$  and  $y_0$ , respectively. The major and minor radii of the ellipse are  $a$  and  $b$ , respectively. Angle  $\theta$  is the angle that the major axis makes with the  $x$ -axis, or the beating angle. A schematic representation of these parameters is shown in the right panel of **Figure 4A**. The fitting is carried out using Igor Pro software by defining the explicit function described above. Then, a histogram of beating angle  $\theta$  for all cilia observed in the same cell is plotted as a circular histogram (**Figure 2** in Narita *et al.*<sup>8</sup>). The frequency is normalized to the number of analyzed ciliary tips. It should be noted that each cilium is interpreted to have two  $\theta$  values in the circular histogram, e.g.  $\pi/4$  and  $3\pi/4$ , leading to symmetrical distribution of the direction.

To define generalized aspect ratio  $AR$ , the positions of the ciliary tip during multiple cycles are rotated by  $-\theta$  (**Figure 4B**). According to the rotation, both back-and-forth and rotational trajectories become distributed approximately parallel to the  $x$ -axis, in which the widths of distribution  $A$  and  $B$ , along the  $x$ - and  $y$ -axes, respectively, are defined as half of the difference between the minimum and maximum. Therefore, these parameters are more relevant to the major and minor radii of the ellipse,  $a$  and  $b$ .  $AR$  is then defined as the ratio between  $A$  and  $B$  by  $AR = B/A$ .

#### Observations of choroid plexus epithelium by SEM

SEM allows observation of the fine surface structure of specimens. The presence of cilia on CPECs is confirmed throughout the developmental time course. The emergence of multiple cilia on CPECs is observed by embryonic day (E) 13, shortly after choroid plexus development begins in the lateral ventricles around E11. At this stage, the cells are small with a variable immature appearance, and the ciliary tips are pointing toward various directions. At E15, a tuft of multiple cilia is established on the top of the apical surface, which are standing out from the surrounding microvilli. At postnatal day (P) 2, many cilia are fixed at a bent position, reflecting the ciliary motility observed by live imaging. At P14, most cells possess multiple cilia that are non-motile as well as microvilli with a finer texture compared with the earlier stages. **Figure 5** shows SEM images of CPECs with cilia at these stages. Based on the movies shown in **Figure 1** and **Movie 1**, it is obvious that motile cilia are easily recognized by live imaging. However, it is difficult to distinguish non-motile cilia by DIC microscopy. Consequently, SEM is indispensable to understand overall ciliary states.

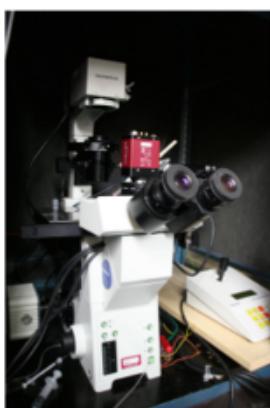
## CPEC preparation

a



live imaging

b



sample processing for SEM

d

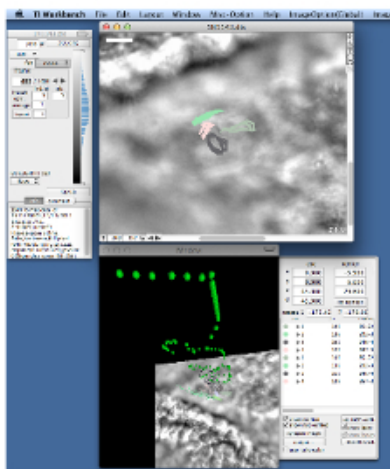


e



image analysis

c



SEM imaging

f

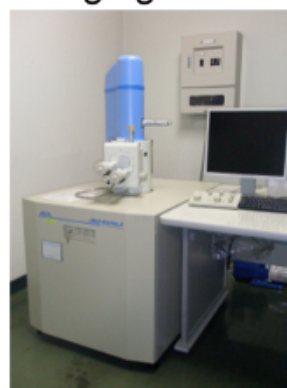


**Figure 1: Overview of the workflow.** (a) Stereo microscope. (b) Inverted microscope equipped with a charged-coupled device (CCD) camera. (c) Computer screen during analysis. (d) Ion sputter. (e) Specimen for SEM. (f) Scanning electron microscope.

**Movie 1.** Movie of the top view of CPECs and the cilia from a P2 mouse pup in high-speed video microscopy. Because of the irregular surface of the choroid plexus tissue, this snapshot contains both in-focus and out-of-focus planes. The area in the box is expanded and shown in **Movie 2**. Scale bar: 2  $\mu\text{m}$ .

**Movie 2.** Movie of the expanded view of the tissue sample in **Movie 1**. Beating cilia showed either rotational or back-and-forth movements. Scale bar: 1  $\mu\text{m}$ .

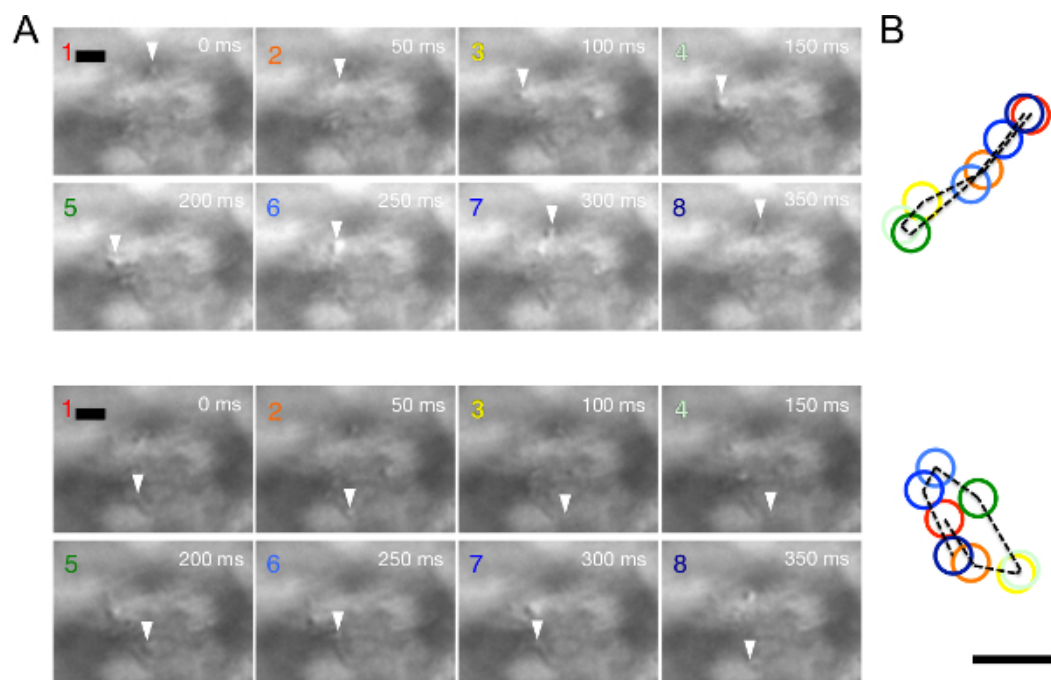


**Figure 2: Reconstitution of the trajectory of CPEC cilia from the time-lapse images in Movie 2.** (A) Cilia with back-and-forth movement (top) and rotational movement (bottom). DIC images from the movie data are presented at 50 msec intervals (1–8, scale bar: 1  $\mu$ m). The position of the target ciliary tip is indicated by an arrowhead. (B) The trajectories (broken line) and positions of ciliary tips (colored circles) shown in images are overlaid.



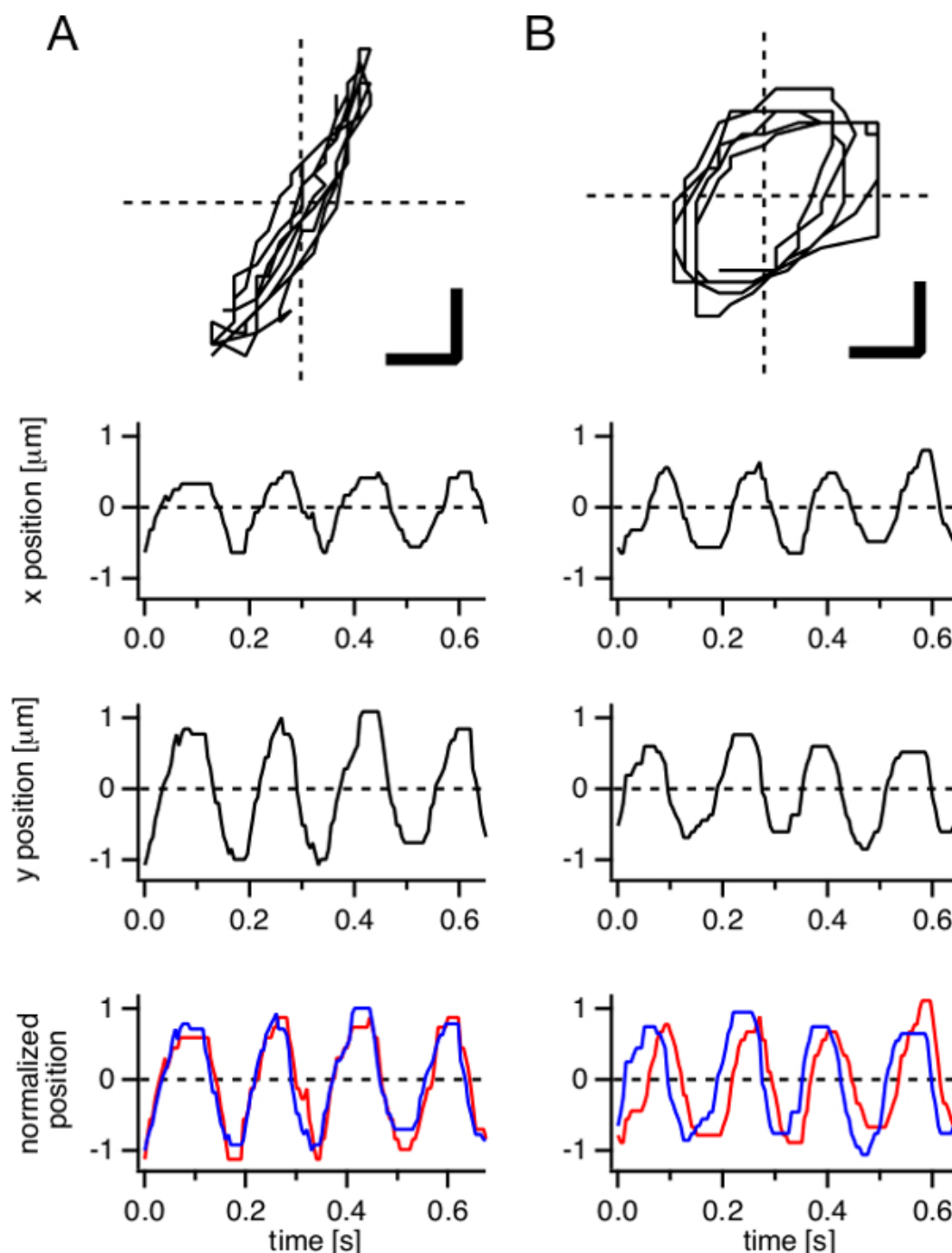


**Figure 3: Two modes of CPEC ciliary tip movement reconstituted from movie data.** Representative ciliary tip movements, back-and-forth movement (A) and rotational movement (B), over multiple cycles are presented as trajectories (top, scale bars: 0.5  $\mu\text{m}$ ). Time courses of x- and y-coordinates of the tip position are plotted, respectively (middle). To demonstrate a phase-shift between the two coordinates, x- and y-coordinates were normalized to [-1,1] and overlaid (bottom, red and blue lines, respectively).

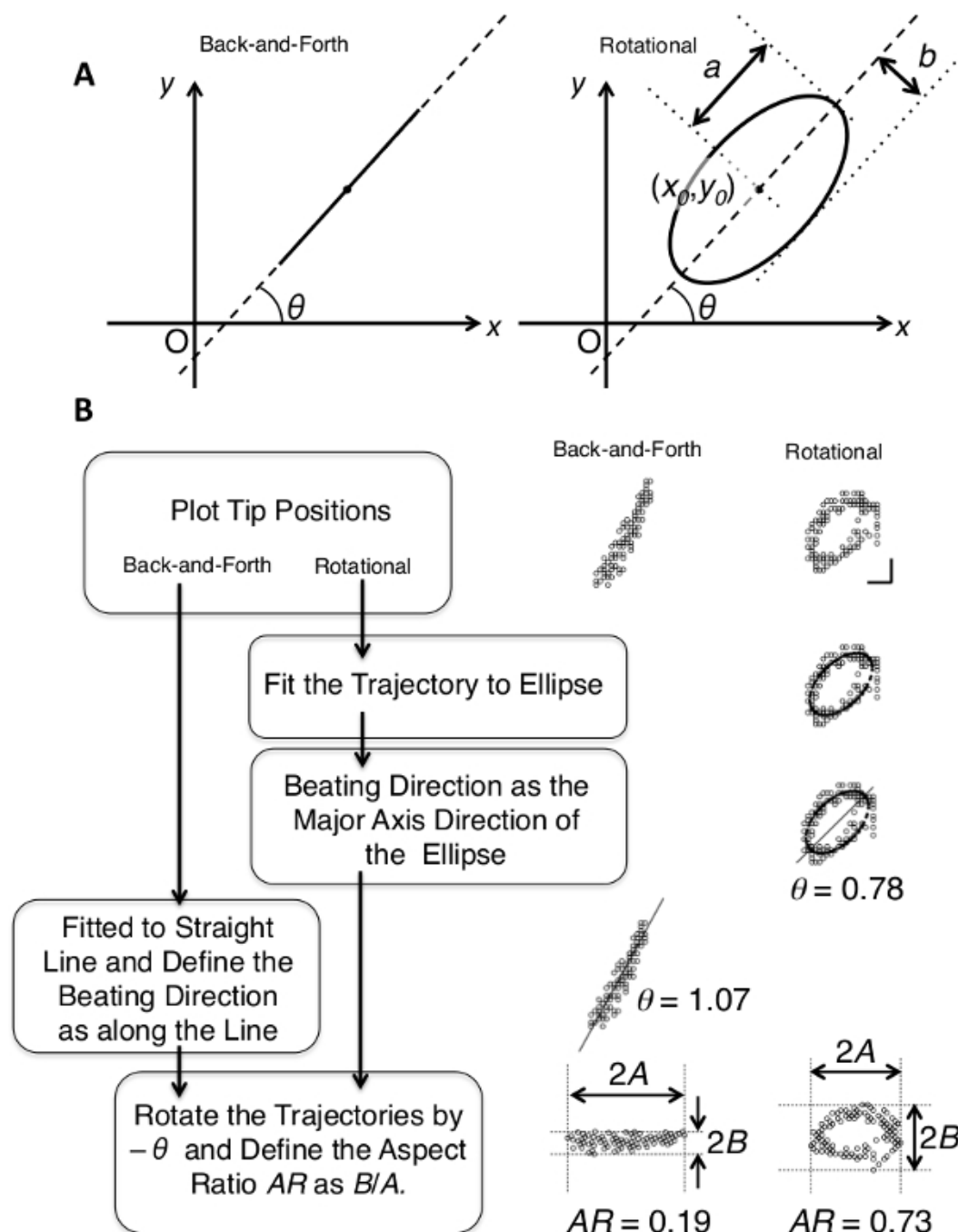


**Figure 4: Schematic illustrations describing the analysis of ciliary tip trajectories.** (A) Definitions of the beating angle  $\theta$  for back-and-forth (left panel) and rotational (right panel) trajectories. Parameters in the formula describing the fitted ellipse,  $a$ ,  $b$ ,  $x_0$ , and  $y_0$ , are shown in the right panel. (B) Flow chart of the fitting analysis of the trajectories to define the beating angle  $\theta$  and  $AR$ . Actual results of the fitting of the representative trajectories are presented in the right panels.



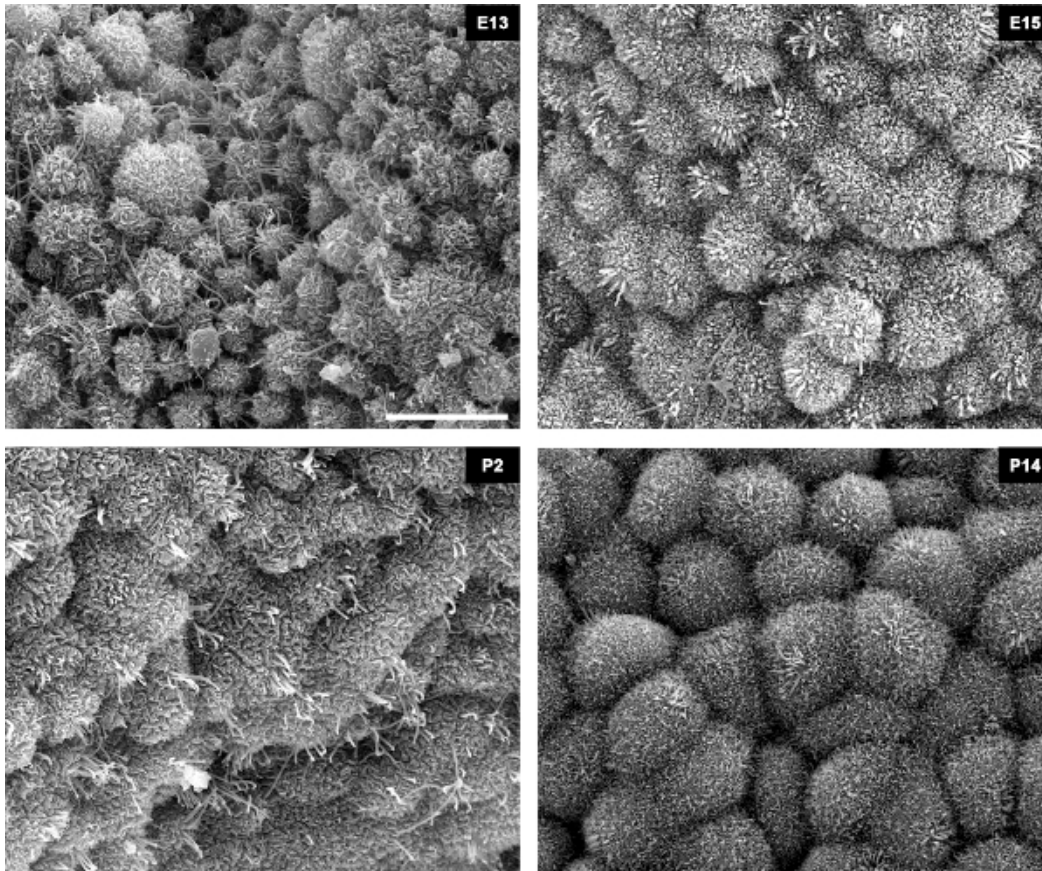


**Figure 5: SEM image of cilia. Representative SEM micrographs of CPECs at E13, E15, P2, and P14.** During the time course, CPECs increased in size, and developed microvilli and cilia on the apical surface. A tuft of cilia at E13 is yet to acquire motility. At P2, when the ratio of cilia with motility reached the highest point, many bent cilia are observed. At P14, cilia lose motility. Scale bar: 5  $\mu$ m.

## Discussion

### Perspectives of this method

Although the technique described here does not provide a more detailed analysis of cilia than previously published methods, the significance of this technique resides in the simplicity of the system and cost effectiveness, which can be easily applied to screening any kind of ciliary motility *ex vivo*. In particular, TI Workbench provides a simple and user-friendly interface that enables researchers to observe and analyze ciliary motility more easily. Effective automated tracking methods have not been developed for low contrast objects such as unstained cilia in video-enhanced contrast-DIC. Although the method to track ciliary motion is manual in this technique, the amount of effort in ciliary motion tracking analysis is optimally reduced compared with using general purpose software packages for image analysis.

### Sample dissection

To prepare *ex vivo* CPEC samples, rapid and gentle manipulations are necessary to preserve the viability of the tissues, which ensures the motility of the cilia *ex vivo*. Because contamination by erythrocytes blurs the field of observation, gentle but intricate rinsing of the dissected tissue with phosphate buffered saline is strongly recommended. To avoid bleeding, care must be exercised to avoid tearing the posterior choroid artery that can be identified as a prominent reddish thread-like structure adhered to the lamina affixa of the colloid plexus.

### Microscope

An inverted microscope equipped with DIC optics and a high-power transmission light source is essential for this method. Because mercury lamps are usually incapable of frequently switching on and off, a shutter in front of the lamp housing is necessary. Either a manual or electrical shutter can be used for this purpose. To protect specimens and the observer's eyes from UV and IR light, optical filters are required to allow only visible light (400–700 band pass or a combination of UV and IR cut filters). ND filters are also necessary to alter the light power that differs according to the situation: monitoring by eye, focusing with a video camera, and high-speed time-lapse recording. An objective lens with a high numerical aperture is necessary for a high resolution. There is some distance between the top of the coverslip and the focal point because of the morphology and thickness of the tissue. Therefore, a water immersion lens rather than an oil immersion lens is preferred for better image quality. Vibration isolation is also necessary to yield stable image stacks. Air dumper-type tables are useful for this purpose, but simpler cushioning of the microscope by inserting tennis balls beneath the microscope base with a steady table may also work.

### Video camera

A CCD camera capable of at least 200 frames/sec is necessary to track the movement of cilia. During the past decade, CCD cameras with faster frame rates than the standard video rate (25–30 Hz) have become available at much lower costs. Camera models capable of shorter exposure times than the frame interval are useful to reduce blurring due to the movement of cilia without increasing the amount of data. An exposure time of 0.1 msec and a 5 msec frame interval (200 Hz) are minimum conditions to obtain ciliary images of CPECs with sufficient quality.

## Software

The analysis to track the motion of each cilium is time consuming, especially when general purpose software packages for image analysis are used to track each ciliary tip. Reducing the steps of repeated tasks, such as mouse clicking on the ciliary tip position on the monitor, selecting a menu to record the clicked position, and clicking on a button to move to next image frame, results in a significant reduction of time and effort. In this study, a special routine was added to the custom-made TI Workbench software. In the ciliary tracking mode of the TI Workbench software, the user keeps looping the following simple two-step operation: moving the mouse pointer to the ciliary tip and pressing an arrow key on the keyboard to advance the frame, which does not require moving the mouse pointer or the user's eyes to shift (to menus and buttons on the computer screen) from the ciliary tips on the computer screen. The software keeps track of the ciliary tip positions, displays the recorded trajectory to assist the user, and creates a table of ciliary motion information for further analysis. Most general purpose software for image analysis permits programming macros for batch processing of such repeated tasks. Such custom programming to reduce repeated steps is strongly recommended.

## Analysis of trajectories

Extraction of the trajectories was carried out using the custom-made TI Workbench software, as described above. Relatively simple analysis and image processing were also carried out using the same software. For fitting analyses, the trajectory of each ciliary tip was transferred to Igor Pro software. Other advanced analysis software such as MATLAB can also be used for this purpose.

In the current study, because of difficulties in categorizing the trajectories into back-and-forth or rotational trajectories, the trajectories were classified by eye in a blinded fashion, which were confirmed by another observer, resulting in consistent classification. Nevertheless, more mathematically rigorous measures to categorize the trajectories without any possible arbitrariness would be preferable. Ellipse fitting of the trajectories appears to be ideal, which could quantify the extent of ellipticity as the aspect ratio of the fitted ellipse ( $\epsilon$ ) in both back-and-forth and rotational movements. However, an attempt to use the distribution of the aspect ratio to define a threshold value for classification was ineffective. The fitting often failed for back-and-forth trajectories, the parameters frequently failed to converge, and the converged fitting was apparently illusive. Therefore, ellipse fitting was not adopted to automatically categorize the trajectories or quantify the ellipticity of each trajectory. The fitting was carried out to extract the beating direction of rotationally moving tips as the major axis of the fitted ellipse.

In the current study, AR was proposed to quantify the extent that a trajectory deviates from an ideal linear back-and-forth motion. The parameter is the ratio of the width of distribution perpendicular to the beating direction to that along the direction. The value should be zero when the trajectory is a straight line, and one when the trajectory is a circle, resembling the aspect ratio of the ellipse mentioned above.

In practice, obtaining the AR value can be relatively easy by rotating the trajectory, so that the beating direction becomes parallel to x-axis (**Figure 4B**). This quantification leads to considerably distinct values for the two modes of motion, suggesting the potential use of the parameter not only to quantify the characteristics of each trajectory, but also to more rigorously classify the trajectories. However, it should be noted that the beating direction itself is already the result of distinct fitting processes for the two modes in the current method.

Further improvement of the analysis, such as a more advanced fitting algorithm, might solve the problems of possible arbitrariness.

An aspect regarding the ellipticity of the trajectory is that the beating of each CPEC cilium may not be taking place in the plane that is strictly perpendicular to the x-y plane of observation. In fact, the results of SEM imaging implied that CPEC cilia are often tilted, and the tilt may lead to apparent ellipticity or anisotropy of the trajectories.

## Preparation for SEM

During the preparation for SEM observation, there are several important points that ensure the acquisition of high quality images. First, post-fixation by osmium tetroxide must be performed carefully, including pre-washing with a 10% sucrose solution. Without proper fixation by the osmification procedure, the subsequent steps cannot maintain or restore the condition of the specimens, leading to a lower quality of the preparation. Because aldehyde fixatives are reducing agents, any remaining aldehydes within the specimen inhibit the activity of osmium tetroxide, a strong oxidizing reagent. To ensure elimination of superfluous aldehydes in specimens, careful washing with the sucrose solution is imperative. In cases of suboptimal post-fixation, the color of the specimen does not change from brown to black. Second, the volume of osmium tetroxide must be at least 50-fold larger than that of the sample. Otherwise, sufficient fixation cannot be expected. Third, it is important to avoid complete drying of the specimens, particularly during the dehydration process that employs highly pure ethanol and isoamyl acetate. Drying of the specimen destroys the fine surface structures such as cilia, resulting in poor images.

## Disclosures

The authors declare that they have no competing financial interests. This paper aims at reporting detailed methodology to observe the motility of cilia in isolated choroid plexus tissues. Scientific novelties have been reported in previous studies<sup>1,8</sup>.

## Acknowledgements

This work was supported by a Project for Private Universities: matching fund subsidy from the Ministry of Education, Culture, Sports, Science and Technology (MEXT) of Japan (T.I.) and Grants-in-Aid for Scientific Research (C) from MEXT (S.T. and K.N.).

## References

1. Nonami, Y., Narita, K., Nakamura, H., Inoue, T., Takeda, S. Developmental changes in ciliary motility on choroid plexus epithelial cells during the perinatal period. *Cytoskeleton*. **70**, (12), 797-803 (2013).
2. Bisgrove, B. W., Yost, H. J. The roles of cilia in developmental disorders and disease. *Development*. **133**, (21), 4131-4143 (2006).
3. Fliegauf, M., Benzing, T., Omran, H. When cilia go bad: cilia defects and ciliopathies. *Nature Reviews. Molecular Cell Biology*. **8**, (11), 880-893 (2007).
4. Oh, E. C., Katsanis, N. Cilia in vertebrate development and disease. *Development*. **139**, (3), 443-448 (2012).
5. Shah, A. S., Ben-Shahar, Y., Moninger, T. O., Kline, J. N., Welsh, M. J. Motile cilia of human airway epithelia are chemosensory. *Science(New York, N.Y)*. **325**, (5944), 1131-1134 (2009).
6. Kiprilov, E. N., *et al.* Human embryonic stem cells in culture possess primary cilia with hedgehog signaling machinery). *The Journal of Cell Biology*. **180**, (5), 897-904 (2008).
7. Hirokawa, N., Tanaka, Y., Okada, Y., Takeda, S. Nodal flow and the generation of left-right asymmetry. *Cell*. **125**, (1), 33-45 (2006).
8. Narita, K., Kozuka-Hata, H., *et al.* Proteomic analysis of multiple primary cilia reveals a novel mode of ciliary development in mammals. *Biology Open*. **1**, (8), 815-825 (2012).
9. Takeda, S., Narita, K. Structure and function of vertebrate cilia, towards a new taxonomy. *Differentiation; Research in Biological Diversity*. **83**, (2), S4-S11 (2012).
10. Ikegami, K., Sato, S., Nakamura, K., Ostrowski, L. E., Setou, M. Tubulin polyglutamylation is essential for airway ciliary function through the regulation of beating asymmetry. *Proceedings of the National Academy of Sciences of the United States of America*. **107**, (23), 10490-10495 (2010).
11. Foster, K. W. Analysis of the ciliary/flagellar beating of *Chlamydomonas*. *Methods in Cell Biology*. **91**, 173-239 (2009).
12. Lechtreck, K. -F., Sanderson, M. J., Witman, G. B. High-speed digital imaging of ependymal cilia in the murine brain. *Methods in Cell Biology*. **91**, 255-264 (2009).
13. Okada, Y., Hirokawa, N. Observation of nodal cilia movement and measurement of nodal flow. *Methods in Cell Biology*. **91**, 265-285 (2009).
14. Chilvers, M. A., Rutman, A., O'Callaghan, C. Ciliary beat pattern is associated with specific ultrastructural defects in primary ciliary dyskinesia. *The Journal of Allergy and Clinical Immunology*. **112**, (3), 518-524 (2003).
15. Takeda, S., *et al.* Left-right asymmetry and kinesin superfamily protein KIF3A: new insights in determination of laterality and mesoderm induction by *kif3A*<sup>-/-</sup> mice analysis. *The Journal of Cell Biology*. **145**, (4), 825-836 (1999).
16. Karnovsky, M. J. A formaldehyde-glutaraldehyde fixative of high osmolarity for use in electron microscopy. *The Journal of Cell Biology*. **27**, 137-138A (1965).